

Attenuation law of normal disc galaxies with clumpy distributions of stars and dust

Akio K. Inoue^{*†}

Laboratoire d'Astrophysique de Marseille, Traverse du Siphon, BP8, 13376 Marseille CEDEX 12, France

Submitted on 1 December 2004, first revision on 17 January 2005, second revision on 27 January 2005

ABSTRACT

We investigate the attenuation law seen through an interstellar medium (ISM) with clumpy spatial distributions of stars and dust. The clumpiness of the dust distribution is introduced by a multi-phase ISM model. We solve a set of radiative transfer equations with multiple anisotropic scatterings through the clumpy ISM in a 1-D plane-parallel geometry by using the mega-grain approximation, in which dusty clumps are regarded as very large particles (i.e. mega-grains). The clumpiness of the stellar distribution is introduced by the youngest stars embedded in the clumps. We assume a smooth spatial distribution for older stars. The youngest stars are surrounded by denser dusty gas and suffer stronger attenuation than diffuse older stars (i.e. age-selective attenuation). The apparent attenuation law is a composite of the attenuation laws for the clumpy younger stars and for the diffuse older stars with a luminosity weight. In general, the stellar population dominating the luminosity changes from older stars to younger stars as the wavelength decreases. This makes the attenuation law steep; the composite attenuation rapidly increases from small attenuation for older stars at a long wavelength to large attenuation for younger stars at a short wavelength. The resultant attenuation law of normal disc galaxies is expected to be much steeper than that of starburst galaxies observed by Calzetti et al. Finally, the Calzetti's attenuation law is regarded as a special case with a large density in our framework.

Key words: dust, extinction — galaxies: ISM — galaxies: spiral — ISM: structure — radiative transfer

1 INTRODUCTION

Since the first dust grain condensation in the universe, dust grains have accumulated in the interstellar medium (ISM) of galaxies. This internal dust attenuates the stellar light before it escapes from galaxies. Thus, we need a correction of the internal dust attenuation in order to obtain the intrinsic flux and the spectrum of galaxies. This procedure should be done with an appropriate attenuation¹ law including effects of scatterings and the configuration of dust and stars. Generally, it is different from the extinction laws observed in the Milky Way and Magellanic Clouds; an extinction law corresponds to the attenuation law in a distant uniform screen geometry which is not realistic at all for most galaxies. However, there are many works in which an extinction law is used to correct for the internal dust attenuation.

Observationally, only an average attenuation law of ultra-violet (UV) bright starburst galaxies has been obtained so far (Calzetti et al. 1994, hereafter it is called the Calzetti law, see also Leitherer et al. 2002 and Buat et al. 2002). This is because the UV spectra of galaxies were rare. GALEX (GALaxy Evolution eXplorer; Martin et al. 2005) will change the situation. We will have UV spectra of a lot of galaxies. From the data, we will obtain attenuation laws of various kinds of galaxies.

Theoretically, to study the attenuation law of galaxies is to solve the radiative transfer in a galactic scale. There are several groups studying the galactic radiative transfer (see Calzetti 2001, for a review and references therein). We will present a brief summary for the works about the attenuation law below. Because of the importance of scatterings (e.g., Bruzual et al. 1988), we restrict ourselves to only works which include scatterings.

The attenuation law through a smooth dust and stellar distribution have been examined since the early phase of this topic (Bruzual et al. 1988; Di Bartolomeo et al. 1995; Ferrara et al. 1999; Baes & Dejonghe 2001b). In general, the

^{*} E-mail: akio.inoue@oamp.fr

[†] JSPS Postdoctoral Fellow for Research Abroad

¹ In this paper, we use the term, “attenuation”. However, other terms (e.g., “effective extinction”, “obscuration”) are also used in the literature (Calzetti 2001).

attenuation amount is smaller than that by a distant uniform screen because of the geometric and scattering effects. For example, let us compare a plane-parallel slab where dust and stars are well mixed with the foreground uniform screen which has the same amount of dust as the slab. Obviously, the optical depth from an outside observer to stars close to the surface of the slab is smaller than that of the foreground screen. This is a geometric effect. The scattering effect is that some scattered photons coming into an observer's line of sight compensate a part of the radiation absorbed and scattered out from the line of sight. Therefore, the geometric and scattering effects make the medium less opaque.

The clumpiness of the medium (i.e. dust distribution) is also important as clearly shown by Natta & Panagia (1984). This also makes the medium more transparent than a uniform screen geometry because there are photons escaping from the medium through a less opaque path (Gordon et al. 1997; Városi & Dwek 1999; Gordon et al. 2000; Witt & Gordon 2000; Bianchi, et al. 2000; Pierini et al. 2004). Since such effects are more efficient for shorter wavelengths, the resultant attenuation law usually becomes grayer than the extinction law (distant uniform screen). For example, Gordon et al. (1997) showed that the attenuation law through the clumpy medium with the Small Magellanic Cloud (SMC) type dust (i.e. no prominent feature at 2175 Å) can be very similar to the Calzetti law which is much grayer than the assumed SMC extinction law.

We can also consider the clumpiness of the stellar distribution. As introduced by Silva et al. (1998), young stars may localize in their birth clouds (i.e. molecular clouds). Because of a larger density of the surrounding gas, the radiation from young stars suffers stronger attenuation than that from stars distributed diffusely outside the birth clouds. With this hypothesis (hereafter it is called the age-selective attenuation), Granato et al. (2000) well reproduced the Calzetti law with the Milky Way (MW) type dust (i.e. with the 2175 Å bump). For starburst galaxies, the radiation field is dominated by the young stellar radiation which suffers a featureless and grayer attenuation law expected through a dense medium. Granato et al. (2000) also obtained a different attenuation law for normal galaxies where the diffuse component plays a role. Tuffs et al. (2004) showed that the global attenuation law is a composite of attenuation laws of various stellar components with weights of their fluxes.

However, there has been no study of the attenuation law taking into account the clumpiness for both distributions of dust and stars, except for Bianchi, et al. (2000). Since their analysis is monochromatic, it is not the attenuation law in a strict sense. In real galaxies, the ISM is very clumpy, and the localization of young stars is often observed. Therefore, we should treat the clumpiness for both of stars and dust to develop the investigation of the attenuation law. The current paper executes it for the first time.

This paper also discusses the relation between the clumpiness and the physics of the medium. In the radiative transfer through the clumpy two-phase medium, there are two essential parameters: the density contrast between clumps and the inter-clump medium, and the volume filling fraction of clumps (e.g., Witt & Gordon 1996). We translate these two parameters into more fundamental quantities, the ISM thermal pressure and the mean density, based on the multi-phase ISM model (e.g., Field et al. 1969); we

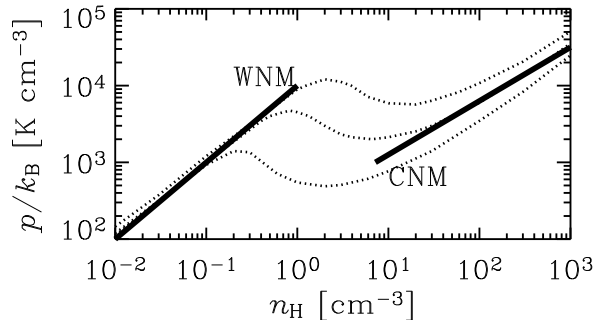


Figure 1. Phase diagram: thermal pressure–hydrogen number density. The dotted curves indicate the thermal equilibrium points in the interstellar medium of the Milky Way (top: Galactocentric radius of 3 kpc, middle: 8.5 kpc, and bottom: 15 kpc) reproduced from fig.7 of Wolfire et al. (2003). The thick solid lines are the approximate relations of two thermally stable phases; the warm neutral medium (WNM, left) and the cold neutral medium (CNM, right). Their analytical forms are given by equations (1) and (2).

try to relate the attenuation law with the ISM physics. Recently, such an attempt was started by Fischera et al. (2003); Fischera & Dopita (2005). Since their analysis was only a distant foreground screen (not uniform but turbulent) case, the geometry considered in this paper is more suitable for extended sources like normal disc galaxies.

This paper is organized as follows: in section 2, we introduce a physical model of the clumpiness as an application of the two-phase ISM model. Then, the radiative transfer and the mega-grain approximation (Városi & Dwek 1999) are described in section 3. The main result of this paper, a steep attenuation law, is presented in section 4. The robustness of the result, the Calzetti law, and a simple prescription of the dust attenuation proposed previously are discussed in section 5. The final section is devoted to the conclusion of this paper.

2 CLUMPINESS OF THE ISM

The ISM in galaxies is very clumpy, and the clumpiness is related with the physics of the ISM. As an application of the multi-phase ISM model (e.g., Field et al. 1969; McKee & Ostriker 1977), a physical model of the clumpiness is introduced in this section.

Assuming thermal energy and chemical equilibria in the ISM with a temperature less than 10^4 K, we find two thermally stable phases in the pressure-density phase diagram (e.g., Wolfire et al. 1995; Koyama & Inutsuka 2000): one is the warm neutral medium (WNM) and the other is the cold neutral medium (CNM). Figure 1 is an example of the phase diagram. The dotted curves indicate the equilibrium points in environments of the Milky Way's ISM calculated by Wolfire et al. (2003). These curves depend on the heating and cooling functions considered; they depend on the metallicity, the dust amount and properties, the intensity of the radiation field, the flux of cosmic rays, and so on. However, differences are apparent mainly in the local maximum and minimum pressures; locations of thermally stable

phases (especially for the WNM) are rather robust. Thus, we adopt the following approximate relations between the thermal pressure and the hydrogen number densities in the two phases:

$$\frac{p/k_B}{10^4 \text{ K cm}^{-3}} = \frac{n_{\text{H,wnm}}}{1 \text{ cm}^{-3}} \quad (\text{WNM}), \quad (1)$$

and

$$\frac{p/k_B}{10^{4.5} \text{ K cm}^{-3}} = \left(\frac{n_{\text{H,cnm}}}{10^3 \text{ cm}^{-3}} \right)^{0.7} \quad (\text{CNM}). \quad (2)$$

They are shown in figure 1 as thick solid lines.

We also assume a thermal pressure equilibrium among phases. Although the total ISM pressure is dominated by the non-thermal (turbulent motions, magnetic fields, and cosmic rays) pressure (e.g., Boulares & Cox 1990), thermal pressures of warm and cold neutral gases and hot gas are similar observationally, $p/k_B = 10^{3-4} \text{ K cm}^{-3}$ (e.g., Myers 1978). Wolfire et al. (2003) proposed a scenario where the thermal energy and pressure equilibria, and then, the two-phase neutral medium should be established in the Milky Way's ISM even in a turbulent condition. Such equilibria are probably valid for the ISM in other normal disc galaxies, at least as a long term averaged property.

In the radiative transfer through a two-phase medium discussed here, we regard the WNM and the CNM as the inter-clump medium and clumps, respectively. Here, the total filling fraction of the WNM and the CNM is assumed to be unity for simplicity although it is about 0.5 observationally (Heiles & Troland 2003). In fact, the rest $\sim 50\%$ of the volume is filled with the hot ($\sim 10^6 \text{ K}$) gas produced by supernovae. This hot gas determines the thermal pressure of the WNM and the CNM (McKee & Ostriker 1977).

Once an equilibrium thermal pressure in the medium is given, we have the densities of the CNM and the WNM based on equations (1) and (2). In other words, we have the density contrast between clumps and the inter-clump medium. Then, we assume a mean density of the hydrogen nucleus which gives the volume filling fraction of clumps; $f_{\text{cl}} = (n_{\text{H}} - n_{\text{H,wnm}})/(n_{\text{H,cnm}} - n_{\text{H,wnm}})$.

Here, we deal with normal disc galaxies. An equilibrium thermal pressure of $p/k_B = 10^{3.5} \text{ K cm}^{-3}$ (Wolfire et al. 2003, for the solar vicinity) and a mean hydrogen number density of $n_{\text{H}} = 1 \text{ cm}^{-3}$ (Spitzer 1978) are assumed. These values are listed in Table 1 where other quantities assumed later are also summarized. The corresponding density contrast and clump filling fraction are 118 and 1.85×10^{-2} , respectively. This density contrast is similar to that considered in Witt & Gordon (2000), whereas our filling fraction is about an order of magnitude smaller than theirs. That is, our mean density of the medium is much less than that in Witt & Gordon (2000).

Finally, clumps are assumed to be self-gravitating; the clump size, which is required to calculate the optical depth of each clump later, is given by the equilibrium pressure and the CNM density through the Jeans length. This is an assumption motivated by the following discussion where we regard clumps as birth clouds of young stars. Indeed, the molecular clouds should be in the CNM. For the equilibrium pressure and mean density assumed above, the Jeans length for a sphere of the CNM is $\sqrt{15p/4\pi G/\rho_{\text{cl}}} = 10.4 \text{ pc}$ ($= r_{\text{cl}}$), where p is the thermal pressure, G is the gravitational constant, and the density inside clumps $\rho_{\text{cl}} = \mu m_{\text{p}} n_{\text{H,cnm}}$

Table 1. Physical quantities determining the attenuation law.

Name	Notation	Standard value
equilibrium thermal pressure	p/k_B	$10^{3.5} \text{ K cm}^{-3}$
mean hydrogen density	n_{H}	1 cm^{-3}
dust-to-gas mass ratio	\mathcal{D}	10^{-2}
half height of the gas+dust disc	h_{d}	150 pc
layering parameter of old stars	ξ	0.5
young stellar age criterion	t_{y}	10^7 yr
homogeneous visual optical depth (face-on)		0.54

with the mean atomic weight $\mu = 1.4$ and the proton mass m_{p} . This size is similar to (but slightly larger than) a typical size of the molecular clouds (e.g., Larson 1981).

3 RADIATIVE TRANSFER

3.1 Dust properties

In this paper, we use an empirical set of dust optical properties taken from Witt & Gordon (2000). This data set consists of the dust opacity ($k_{\text{d},\lambda}$), the scattering albedo ($\omega_{\text{d},\lambda}$), and the asymmetry parameter ($g_{\text{d},\lambda}$) for the MW type and the SMC type dust. The number of wavelengths is 25 from $0.1 \mu\text{m}$ to $3 \mu\text{m}$. Since there is only the wavelength dependence for $k_{\text{d},\lambda}$ in the data set, we adopt the absolute value of the opacity at visual band as $k_{\text{d},\text{V}} = 2.5 \times 10^4 \text{ cm}^2 \text{ g}^{-1}$ (extinction cross section per unit dust mass; e.g., Draine 2003) for both types of dust although the actual values for the MW dust and the SMC dust are slightly different. Effects of the size distribution and the composition are already included in the data. For calculations of the scattering angle, we assume the Henyey-Greenstein phase function (Henyey & Greenstein 1941) for simplicity although Draine (2003) proposed a better function. Finally, we assume the dust-to-gas mass ratio in the ISM of the Milky Way $\mathcal{D} = 10^{-2}$ (e.g., Spitzer 1978), as a standard value.

3.2 Mega-grain approximation

To treat clumpiness in the radiative transfer problem, we have to consider a spatial 3-D geometry. However, we can do in a spatial 1-D geometry with the mega-grain approximation introduced by Neufeld (1991); Hobson & Padman (1993) and further developed by Városi & Dwek (1999). In this approximation, we regard a dusty clump as a huge particle called a mega-grain which produces absorption and scattering effects like a normal dust grain. Practically, we replace usual optical properties of normal dust grains (extinction coefficient, albedo, and asymmetry parameter) with effective ones. We follow the formulation given by Városi & Dwek (1999), in which an extensive comparison between the approximation and 3-D Monte-Carlo radiative transfer calculations has been made in some spherical geometries and the validity of the approximation has been shown clearly. We give a summary of equations used in this paper below. We will omit to write the wavelength dependence explicitly.

We assume that all clumps are an identical sphere with the radius r_{cl} and the gas density ρ_{cl} given in section 2 and these clumps are floating in the inter-clump medium with

the gas density $\rho_{\text{icm}} = \mu m_{\text{p}} n_{\text{H,wnm}}$. The optical depth (radius) of a clump relative to the inter-clump medium is

$$\tau_{\text{cl}} = (\rho_{\text{cl}} - \rho_{\text{icm}}) k_{\text{d}} \mathcal{D} r_{\text{cl}}. \quad (3)$$

This optical depth vanishes in the case of no density contrast. Since the interaction (absorption and scattering) probability against the parallel light by a sphere with an optical depth (radius) τ is exactly

$$P_{\text{int}}(\tau) = 1 - \frac{1}{2\tau^2} + \left(\frac{1}{\tau} + \frac{1}{2\tau^2}\right) e^{-2\tau}, \quad (4)$$

the extinction coefficient per unit length of the medium by clumps (i.e. mega-grains) is

$$\kappa_{\text{mg}} = n_{\text{cl}} \pi r_{\text{cl}}^2 P_{\text{int}}(\tau_{\text{cl}}) = \frac{3f_{\text{cl}}}{4r_{\text{cl}}} P_{\text{int}}(\tau_{\text{cl}}), \quad (5)$$

where the clump number density n_{cl} was replaced with $3f_{\text{cl}}/4\pi r_{\text{cl}}^3$. We did not consider any overlap of clumps. Then, the effective extinction coefficient per unit length in the two-phase medium is defined as

$$\kappa_{\text{eff}} = \kappa_{\text{mg}} + \kappa_{\text{icm}}, \quad (6)$$

where $\kappa_{\text{icm}} = k_{\text{d}} \mathcal{D} \rho_{\text{icm}}$ is the extinction coefficient per unit length of the inter-clump medium.

The effective albedo ω_{eff} and the effective asymmetry parameter g_{eff} are also defined as

$$\omega_{\text{eff}} = \frac{\omega_{\text{cl}} \kappa_{\text{mg}} + \omega_{\text{d}} \kappa_{\text{icm}}}{\kappa_{\text{eff}}}, \quad (7)$$

and

$$g_{\text{eff}} = \frac{g_{\text{cl}} \kappa_{\text{mg}} + g_{\text{d}} \kappa_{\text{icm}}}{\kappa_{\text{eff}}}, \quad (8)$$

respectively, where ω_{cl} and g_{cl} are the albedo and asymmetry parameter of a clump, respectively. Városi & Dwek (1999) proposed an expression of ω_{cl} as

$$\omega_{\text{cl}} = \omega_{\text{d}} P_{\text{esc}}(\tau_{\text{cl}}, \omega_{\text{d}}), \quad (9)$$

where

$$P_{\text{esc}}(\tau, \omega) = \frac{(3/4\tau) P_{\text{int}}(\tau)}{1 - \omega[1 - (3/4\tau) P_{\text{int}}(\tau)]}. \quad (10)$$

This is the photon escape probability from a sphere in which isotropic sources and dust whose scattering is isotropic distribute uniformly. In the derivation of equation (10), the uniform distribution of the scattered photons is also assumed (see Appendix C of Városi & Dwek 1999). Although equation (9) is an approximation, the agreement with results obtained by the Monte Carlo simulation is good (Városi & Dwek 1999). For the clump asymmetry parameter, we use equation (43) of Városi & Dwek (1999) which is an analytical fitting formula of their Monte Carlo simulation results.

In the case with a large filling fraction of clumps f_{cl} , the overlap of clumps happens. Városi & Dwek (1999) proposed the replacement of r_{cl} with $r_{\text{cl}}(1 - f_{\text{cl}})^\gamma$ to take into account this overlap effect. Városi & Dwek (1999) also noted that $\gamma = 1$ is suitable for the case of uniformly distributed sources which is our case. Although it is included in the computation, this effect is almost negligible for the standard case discussed later because $f_{\text{cl}} \ll 1$.

3.3 Transfer equations

Suppose a 1-D plane-parallel geometry along z -axis. The mid-plane is set to be $z = 0$ where we put a mirror boundary. Above the mid-plane, we put the gas+dust disc with a constant mean density up to a height of h_{d} . Here, we assume $h_{\text{d}} = 150$ pc which is the observed height of the cold neutral and molecular gas in the Milky Way (e.g., Binney & Merrifield 1998). Although its mean density is constant, it has a clumpy structure described in section 2, and its extinction coefficient is the effective one κ_{eff} given by the mega-grain approximation. For simplicity, we assume that there is no dust outside the gas+dust disc. Then, the optical depth coordinate is defined as $d\tau = -\kappa_{\text{eff}} dz$ with $\tau = 0$ at $z = h_{\text{d}}$. Since κ_{eff} is constant throughout the gas+dust disc, we have $\tau = \kappa_{\text{eff}} h_{\text{d}}$ at $z = 0$. Note that the effective albedo ω_{eff} and the effective asymmetry parameter g_{eff} are also constant throughout the disc.

A static radiative transfer equation in this geometry is

$$\mu \frac{dI(\tau, \mu)}{d\tau} = S(\tau, \mu) - I(\tau, \mu), \quad (11)$$

where I is the specific intensity along a ray and μ is the cosine of the angle between the ray and the z -axis. The source function S is given by

$$S(\tau, \mu) = \eta_*(\tau)/\kappa_{\text{eff}} + \omega_{\text{eff}} \int_{-1}^1 I(\tau, \mu') \Phi(g_{\text{eff}}, \mu, \mu') d\mu', \quad (12)$$

where η_* is the stellar emissivity (isotropic) and Φ is the scattering phase function. Note that ω_{eff} and g_{eff} appear in the second term of the right hand side (i.e. scattering term). The boundary conditions are

$$I(\tau = \kappa_{\text{eff}} h_{\text{d}}, \mu) = I(\tau = \kappa_{\text{eff}} h_{\text{d}}, -\mu), \quad (13)$$

at $z = 0$ (mirror boundary) and

$$I(\tau = 0, \mu < 0) = -\frac{I_*}{\mu}, \quad (14)$$

at $z = h_{\text{d}}$, where

$$I_* \equiv \int_{h_{\text{d}}}^{\infty} \eta_*(z) dz. \quad (15)$$

3.4 Emissivity distribution — Stellar clumpiness

We consider two kinds of the emissivity source: one is embedded in clumps and the other distributes diffusely and smoothly. Then, we consider that the embedded source is the youngest stars (the age criterion is defined later) and other older stars distribute diffusely. This is motivated by the fact that stars are formed in molecular clouds (i.e. clumps) and diffuse as ageing. This makes the clumpiness of the emissivity. Here we normalize the intrinsic (i.e. in the no dust case) emissivity of each component as

$$\int_{-\infty}^{\infty} \eta_*(z) dz = 1. \quad (16)$$

3.4.1 Clumpy stellar emissivity

When clumps distribute uniformly in the gas+dust disc (we did not consider any spatial correlation of clumps in section 2), a mean density of stars embedded in clumps is constant

throughout the gas+dust disc. On the other hand, there is no embedded star outside the disc because there is no clump. Thus, the intrinsic clumpy stellar emissivity is $1/2h_d$ for $|z| \leq h_d$ and zero for $|z| > h_d$ when it is normalized as equation (16). A part of the radiation energy from the embedded stars is locally absorbed by dust in a clump. If stars distribute in the clump uniformly and the scattering by dust is isotropic, we can adopt the escape probability of equation (10). Therefore, the clumpy stellar emissivity input into the transfer equation is

$$\eta_*(z) = \begin{cases} P_{\text{esc}}(\tau_{\text{cl}}, \omega_{\text{cl}})/2h_d & (\text{for } |z| \leq h_d) \\ 0 & (\text{for } |z| > h_d) \end{cases}. \quad (17)$$

In this case, we have $I_* = 0$.

3.4.2 Diffuse stellar emissivity

The diffuse stellar disc is assumed to have an exponential structure along z -axis with a scale height of h_d/ξ , where ξ is the layering parameter, i.e. the ratio of the heights of the dusty disc to the stellar disc. Here we set $\xi = 0.5$ which means that the stellar scale height is twice times larger than the height of the gas+dust disc (e.g., Binney & Merrifield 1998). From the normalization of equation (16), we have

$$\eta_*(z) = \frac{\xi e^{-\xi|z|/h_d}}{2h_d}. \quad (18)$$

In this case, $I_* = e^{-\xi}/2$.

3.5 Computational scheme

The radiative transfer equation described above was solved by the Λ -iteration scheme with a difference formula of the formal solution (e.g., Mihalas & Weibel-Mihalas 1999). The iteration was continued until the maximum fractional difference between previous and present values of S becomes less than 10^{-10} . To accelerate the convergence, we adopted the Ng's algorithm (Ng 1974; Olson et al. 1986). Thanks to a modest optical depth of the problem discussed here, the number of iterations was always less than 10–20 times.

As a code test, we compared the inclination dependences of the attenuation amount for several optical bands in a smooth plain-parallel geometry calculated by the radiative transfer code of this paper with that calculated by a spherical harmonics method presented in table 2 of Baes & Dejonghe (2001a). For the comparison, we adjusted the code to the set up of Baes & Dejonghe (2001a). The agreement was excellent: differences were within a few % in magnitude.

3.6 Transmission rate

We first define the transmission rate for each emissivity source. The intensity observed by a distant observer (in a direction $\mu > 0$) is

$$I_{\text{obs}}(\mu > 0) = I(\tau = 0, \mu > 0) + \frac{I_*}{\mu}. \quad (19)$$

On the other hand, the intrinsic (no dust case) intensity to the observer is

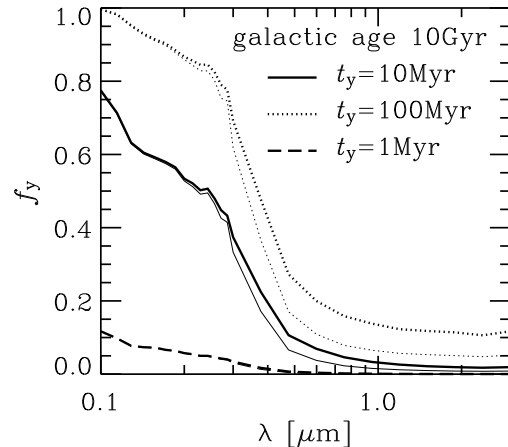


Figure 2. Luminosity fraction of young stellar population as a function of the wavelength at the galactic age of 10 Gyr. The solid, dashed, and dotted curves are the cases with the age criterion for young stars of 10 Myr, 1 Myr, and 100 Myr, respectively. A constant star formation history is assumed for thick curves, and an exponentially decaying star formation history with 5 Gyr time-scale is assumed for thin curves. The difference between the two dashed curves are too small to see it.

$$I_{\text{int}}(\mu > 0) = \frac{1}{\mu}, \quad (20)$$

because of the normalization of equation (16). Thus, the transmission rate is

$$T(\mu > 0) \equiv \frac{I_{\text{obs}}(\mu > 0)}{I_{\text{int}}(\mu > 0)} = \mu I(\tau = 0, \mu > 0) + I_*. \quad (21)$$

When we consider two components of the emissivity source (clumpy and diffuse), the total transmission rate becomes a composite of transmission rates for them as

$$T = fT_1 + (1 - f)T_0, \quad (22)$$

where f is the fraction of the emissivity embedded in clumps, and

T_1 : The transmission rate for the clumpy source.

T_0 : The transmission rate for the diffuse source.

Hereafter, these abbreviations are used.

Since we consider that the embedded source is the youngest stars and the diffuse source is older stars, T_1 and T_0 are transmission rates for the radiation from younger stars inside clumps and for the radiation from older stars outside clumps, respectively. The emissivity fraction f is now the luminosity fraction of the younger stars. We denote it as f_y . It depends on the star formation history in addition to the age criterion of young stars. If the star formation rate at a galactic age t is denoted by $\Psi(t)$, the luminosity fraction f_y as a function of the age t is

$$f_y(t) = \frac{\int_0^{\min[t_y, t]} \Psi(t - t')L(t')dt'}{\int_0^t \Psi(t - t')L(t')dt'}, \quad (23)$$

where t_y is the criterion of the young stellar population, and $L(t)$ is the luminosity density of the simple stellar population at the age t .

Figure 2 shows the wavelength dependence of f_y for several values of t_y in the galactic age of 10 Gyr case. Al-

though we assumed two star formation histories, a constant star formation rate and an exponentially decaying star formation with 5 Gyr time-scale, the differences are very small. Hereafter, we discuss only the constant star formation case. On the other hand, the choice of t_y is more important.

The age criterion, t_y is physically related with the lifetime of the birth clouds (i.e. clumps) and/or the time-scale of stars moving out from the birth clouds. The lifetime of the molecular clouds is estimated to be about 10 Myr (Blitz & Shu 1980). The moving off time-scale is also about 10 Myr for the size of clumps considered here since the observed velocity dispersion of young stars is ~ 1 km s^{-1} (e.g., de Bruijne 1999). Moreover, Calzetti et al. (1994) found larger attenuation against the hydrogen recombination lines than that against the UV stellar continuum. This implies that ionizing stars (i.e. O-type stars) are more deeply embedded in dusty clouds than later-type stars. The main-sequence life-time of the latest O-type stars is also about 10 Myr. Therefore, we choose 10 Myr as a typical value for t_y (Silva et al. 1998; Charlot & Fall 2000).

4 RESULT: A STEEP ATTENUATION LAW

We first show a typical attenuation law of normal disc galaxies with the standard values of physical quantities summarized in table 1. For comparisons with the literature, we note the equivalent face-on visual optical depth in the homogeneous case:

$$\tau_V^{\text{hom}} = 0.54 \left(\frac{n_H}{1 \text{ cm}^{-3}} \right) \left(\frac{h_d}{150 \text{ pc}} \right) \left(\frac{D}{10^{-2}} \right), \quad (24)$$

for the visual extinction cross section per unit dust mass $k_{d,V} = 2.5 \times 10^4 \text{ cm}^2 \text{ g}^{-1}$.

Figure 3 shows the transmission rates for the face-on ($\mu = 1$) case: the panel (a) is the case assumed the MW type dust (with the 2175 Å bump) and the panel (b) is the case assumed the SMC type dust (without the bump). The solid curves are the cases of the clumpy dust distribution: in each panel, the upper thin curve is the transmission rate T_0 and the lower thin curve is the transmission rate T_1 . The thick solid curve in each panel is the typical case for normal disc galaxies, i.e. the composite transmission rate by equation (22) with f_y displayed as the solid curve in figure 2 ($t_y = 10$ Myr). For a comparison, the uniform screen case and the uniform gas+dust disc case (i.e. no clumpiness for stars and dust) are shown by the dotted and dashed curves, respectively.

Generally the ISM clumpiness makes the medium less opaque. Indeed, the transmission rates increase in order of the screen (dotted), the uniform disc (dashed), and the clumpy disc (upper thin solid, T_0). However, we can have heavier attenuation if stars are embedded in clumps (lower thin solid, T_1) (see also Bianchi, et al. 2000).

The composite transmission rate, T_λ follows $T_{0,\lambda}$ at long wavelengths where old stars outside clumps dominate the luminosity (i.e., $f_{y,\lambda} \simeq 0$), whereas it approaches $T_{1,\lambda}$ at short wavelengths where young stars inside clumps dominate the luminosity (i.e., $f_{y,\lambda} \simeq 1$). This makes the attenuation law steep. As shown in figure 4, the expected typical attenuation law of normal disc galaxies (thick solid curve) is much

steeper than the Calzetti law² (dot-dashed curve), the extinction laws (i.e., uniform screen case, dotted curve) and the attenuation law for the uniform stellar and dust distribution (dashed curve). This is the main conclusion of this paper.

Before moving to the examination of the parameter dependences, we note that the transmission rate slightly larger than unity for a very small opacity case (e.g., longer wavelengths). For the case displayed in figure 3, the transmission rate is 1.004 at 2 μm , that is, 0.4% brighter than the intrinsic luminosity. This is not artefact but real due to the effect of scatterings (e.g., Baes & Dejonghe 2001b, see also section 5.1.7).

5 DISCUSSION

5.1 Robustness of the result

A steep attenuation law obtained in the previous section is mainly caused by the age-selective attenuation; a composite of two different attenuations, namely, smaller attenuation for diffuse stars and larger attenuation for young stars embedded in clumps. Here, we examine which parameters affect on the conclusion by changing values of them from the standard case (table 1) one by one. In figures of this section, we will see only one case of the MW type dust or the SMC type dust because the two dust cases give qualitatively very similar results.

5.1.1 Young stellar age criterion

First we change the criterion of young stars, t_y . As shown in figure 2, it affects on the luminosity fraction of young stars, f_y . Figure 5 shows the effect of t_y on transmission rates and attenuation laws. For the thick solid, dotted, and dashed curves, $t_y = 10$ Myr, 100 Myr, and 1 Myr are assumed, respectively. Two thin solid curves in the panel (a) are transmission rates T_0 (upper) and T_1 (lower). As t_y increases, f_y increases and approaches unity, so that the composite transmission rate decreases and approaches T_1 . On the other hand, the attenuation laws normalized at visual band for $t_y \gtrsim 10$ Myr are very similar. The conclusion of a steep attenuation law is not much affected by t_y if $t_y \gtrsim 10$ Myr. Even for the case of $t_y = 1$ Myr, the attenuation law is steeper than the Calzetti's law.

5.1.2 Layering parameter for diffuse stellar disc

Even if we change the layering parameter for diffuse stellar disc ξ , the resultant transmission rates and attenuation laws are almost not changed as shown in figure 6 where three cases of $\xi = 0.5$ (solid), 1.0 (dotted), and 2.0 (dashed) are displayed. This is because the typical disc considered here is not so opaque (the visual optical depth is about 0.5 in the uniform screen geometry). If we considered an opaque disc, the transmission rate (equation 21) would be determined by the second term which depends on the layering parameter ξ more strongly, so that some differences would appear.

² We extrapolated the attenuation law presented by Calzetti (2001), based on Leitherer et al. (2002) for $\lambda < 0.18\mu\text{m}$.

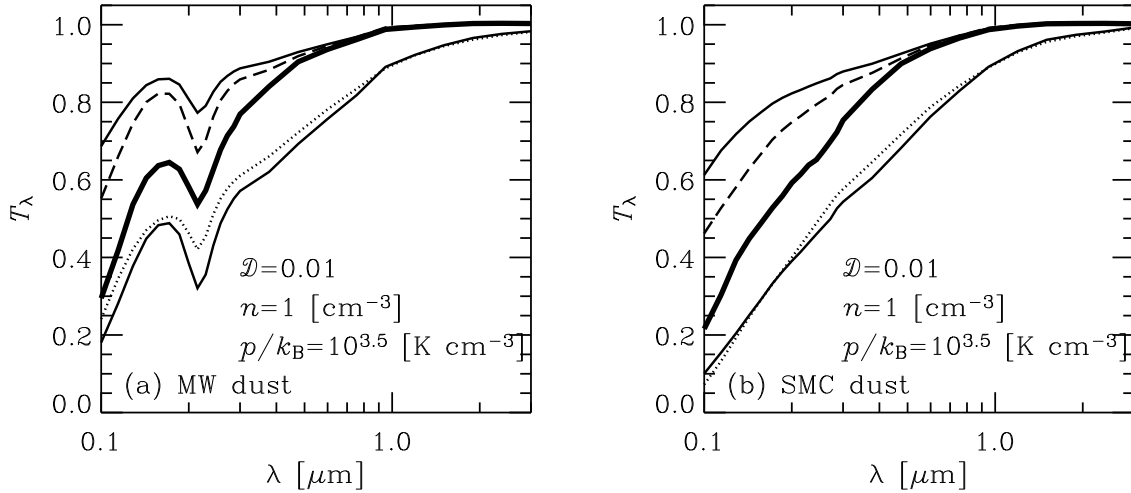


Figure 3. Face-on transmission rates for (a) the Milky Way type dust and (b) the Small Magellanic Cloud type dust. In each panel, the upper thin solid curve is the transmission rate for the source outside clumps (T_0), the lower thin solid curve is that for the source inside clumps (T_1), and the thick solid curve is a composite of the two cases with the luminosity weight f_y displayed as the solid curve in figure 2 (the age criterion of young stars is 10 Myr). The dotted and dashed curves are the uniform screen and the uniform disc (no clumpiness for stars and dust) cases, respectively. The height of the dusty disc is 150 pc and the layering parameter of the diffuse stellar disc is 0.5. Other assumed quantities are displayed in the panels.

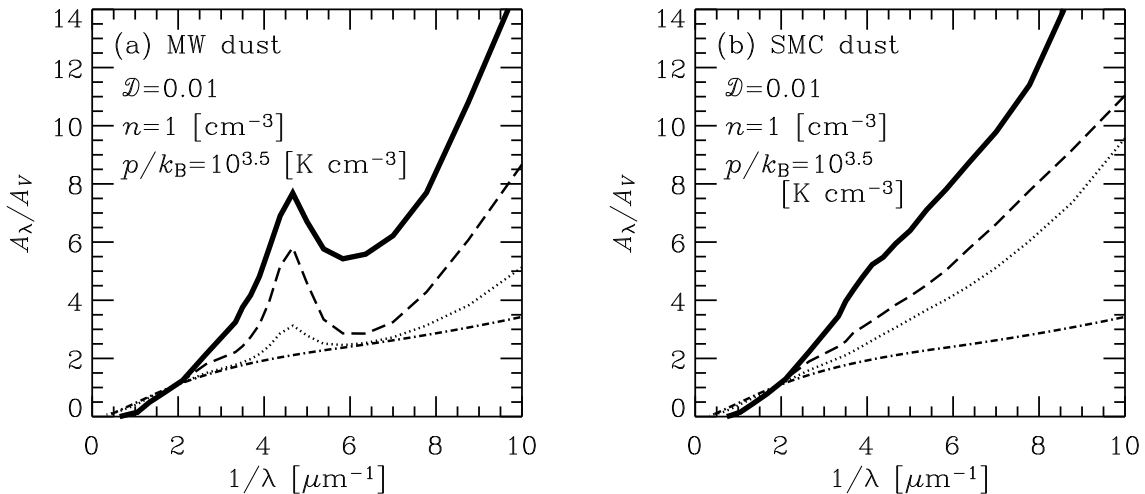


Figure 4. Face-on attenuation laws (normalized at visual band) for (a) the Milky Way type dust and (b) the Small Magellanic Cloud type dust. The solid curve is the typical case for normal disc galaxies denoted as the thick solid curve in figure 3. The dotted and dashed curves are the uniform screen and the uniform disc (no clumpiness for stars and dust) cases, respectively. The dot-dashed curve is the Calzetti law (Calzetti 2001; Leitherer et al. 2002). The height of the dusty disc is 150 pc and the layering parameter of the diffuse stellar disc is 0.5. The criterion of the young stellar age is 10 Myr. Other assumed quantities are displayed in the panels.

5.1.3 Inclination angle

Figure 7 shows the composite transmission rates and attenuation laws for several cases of the inclination angle. As the inclination angle increases (μ decreases), the disc optical depth increases because the disc apparent thickness has a dependence of $1/\mu$. The effect of the disc edge appears from an inclination angle larger than 89° if the ratio of the disc radius to the vertical thickness is 100. However, the radial density structure may affect on a highly inclined case. When we restrict ourselves to a inclination angle of 45° , for

example, the difference from the face-on case is still small, i.e. a steep attenuation law.

5.1.4 Mean gas density

Figure 8 shows the effect of the mean gas density on the composite transmission rates and attenuation laws. To keep the two-phase medium described in section 2, the hydrogen number density is limited in the range of $n_{\text{H,WNM}} \leq n_{\text{H}} \leq n_{\text{H,CNM}}$. As the hydrogen number density increases,

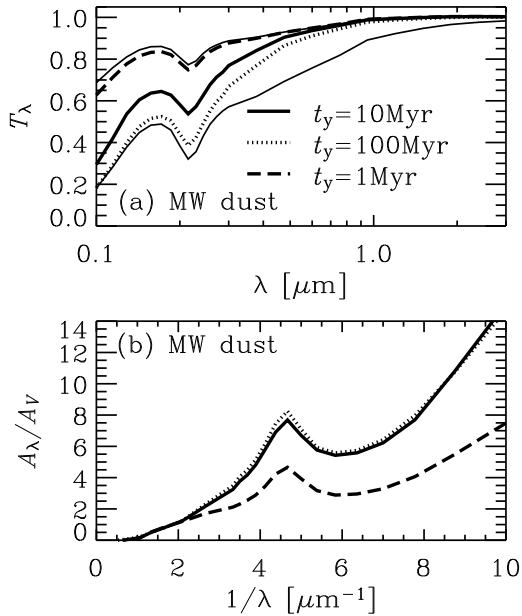


Figure 5. Dependence on the criterion of the young stellar age (t_y): (a) transmission rates and (b) attenuation laws normalized at visual band. In both panels, thick solid, dotted, and dashed curves are the composite transmission rates/attenuation laws with $t_y = 10$ Myr, 100 Myr, and 1 Myr, respectively. Thin solid curves in panel (a) are transmission rates T_0 (upper) and T_1 (lower). The Milky Way type dust is assumed.

the transmission rates decreases and the attenuation laws becomes grayer because the disc optical depth increases.³ For normal disc galaxies, a mean hydrogen number density is typically around 1 cm^{-3} (e.g., Spitzer 1978) in which we expect a steep attenuation law. On the other hand, a larger mean density is expected for actively star-forming galaxies, e.g., UV bright starburst galaxies observed by Calzetti et al. (1994). This means that the Calzetti law can be reproduced by a high density condition. Indeed, this is found in section 5.2.

5.1.5 Equilibrium thermal pressure

When we change the equilibrium thermal pressure, we should direct our attention to the local minimum and maximum pressures. Since we stand on a two-phase ISM model described in section 2, we restrict ourselves within the range between $p/k_B = 10^3 \text{ K cm}^{-3}$ and 10^4 K cm^{-3} expected that a two-phase medium is established in the environment of the Milky Way's ISM (figure 1, see also Wolfire et al. 2003). We show the dependence on the thermal pressure in figure 9 where the mean hydrogen density of 3 cm^{-3} is assumed in order to have a clump filling fraction larger than zero for

³ As increasing the disc optical depth, the transmission rate gradually saturates at I_* in equation (21). If the layering parameter does not depend on the wavelength, the saturation value does not, either. Thus, we have a featureless and gray attenuation law.

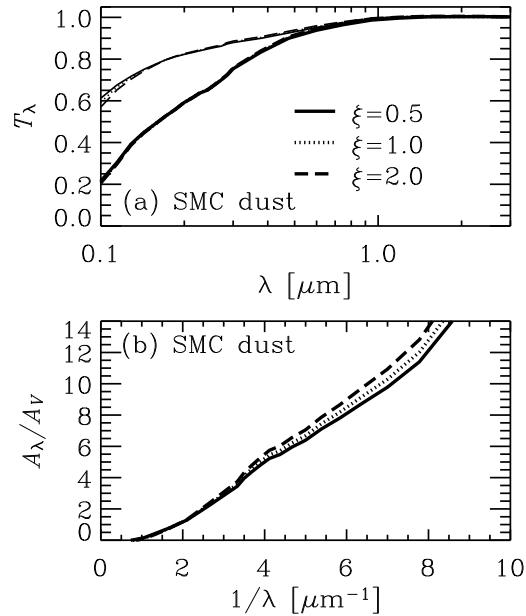


Figure 6. Dependence on the layering parameter for the diffuse stellar disc (ξ): (a) transmission rates and (b) attenuation laws normalized at visual band. In both panels, thick solid, dotted, and dashed curves are the composite transmission rates/attenuation laws with $\xi = 0.5$, 1.0, and 2.0, respectively. In panel (a), thin solid, dotted, and dashed curves are transmission rates T_0 . The transmission rate T_1 is not affected by ξ . The Small Magellanic Cloud type dust is assumed.

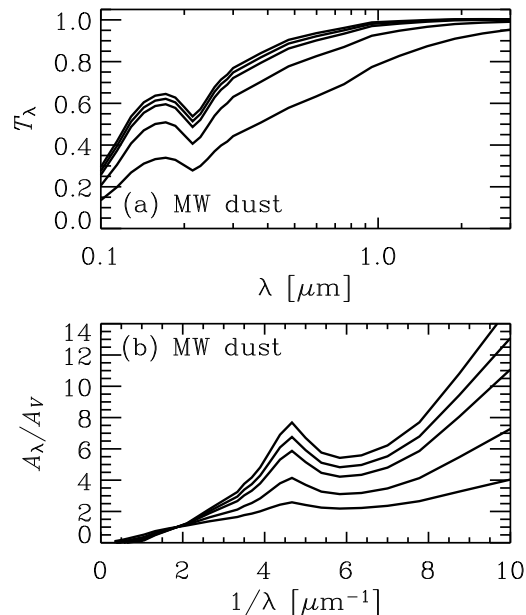


Figure 7. Dependence on the inclination angle: (a) composite transmission rates and (b) composite attenuation laws normalized at visual band. The inclination angle is 0° , 29.4° , 42.1° , 61.1° , and 76.9° from top to bottom in both panels. The Milky Way type dust is assumed.

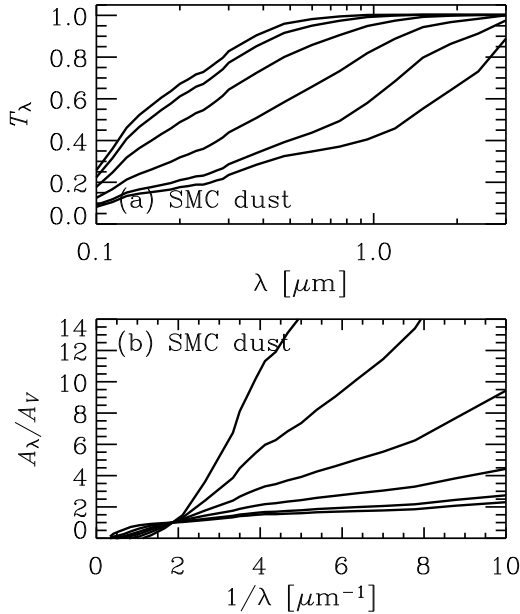


Figure 8. Dependence on the mean gas density: (a) composite transmission rates and (b) composite attenuation laws normalized at visual band. The hydrogen number density is 0.32, 0.82, 2.1, 5.5, 14.4, and 37.3 cm^{-3} from top to bottom in both panels. The Small Magellanic Cloud type dust is assumed.

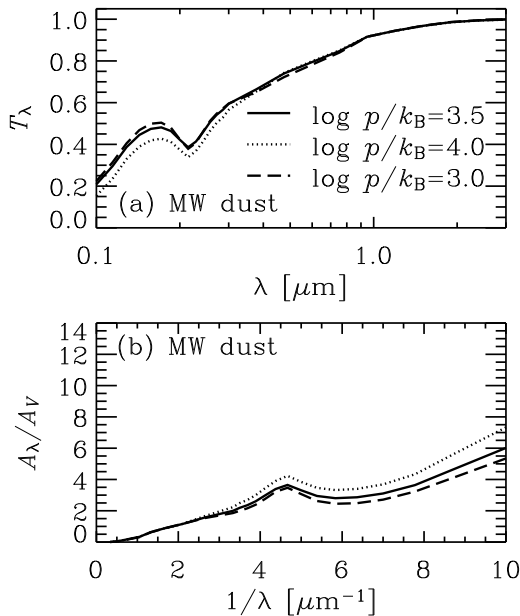


Figure 9. Dependence on the equilibrium thermal pressure (p/k_B): (a) composite transmission rates and (b) composite attenuation laws normalized at visual band. In both panels, solid, dotted, and dashed curves are the cases with $p/k_B = 10^{3.5} \text{ K cm}^{-3}$, $10^{4.0} \text{ K cm}^{-3}$, and $10^{3.0} \text{ K cm}^{-3}$, respectively. The Milky Way type dust and the mean hydrogen density of 3 cm^{-3} are assumed.

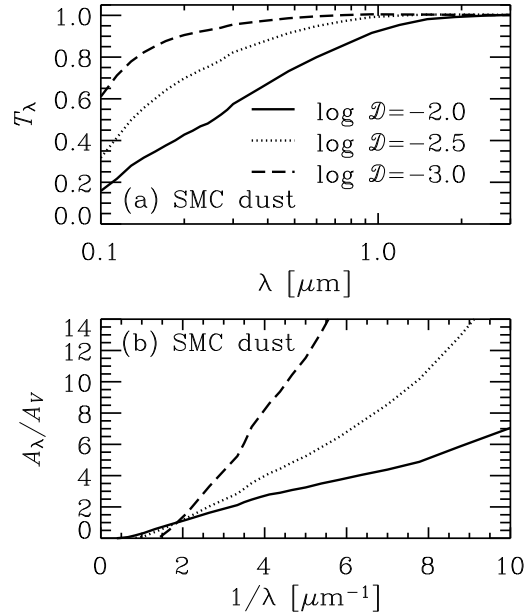


Figure 10. Dependence on the dust-to-gas mass ratio (\mathcal{D}): (a) composite transmission rates and (b) composite attenuation laws normalized at visual band. In both panels, solid, dotted, and dashed curves are the cases with $\mathcal{D} = 10^{-2.0}$, $10^{-2.5}$, and $10^{-3.0}$, respectively. The Small Magellanic Cloud type dust and the mean hydrogen density of 3 cm^{-3} are assumed.

the $p/k_B = 10^3 \text{ K cm}^{-3}$ case. If we adopted the mean density of 1 cm^{-3} , we would have $n_H = n_{H, \text{wnm}}$ (see eq.1), and then, $f_{\text{cl}} = 0$ for the $p/k_B = 10^3 \text{ K cm}^{-3}$ case. The pressure affects on the attenuation law by two ways: the density contrast between clumps and the inter-clump medium, and the clump optical depth through the size (i.e. Jeans length). Approximately, the density contrast is proportional to $p^{0.4}$ found from equations (1) and (2), and the clump optical depth is proportional to $p^{0.5}$ found from equation (3). Thus, the effect of the pressure is not so large as shown in figure 9 for the limited range of the value considered here.

5.1.6 Dust-to-gas mass ratio

Figure 10 shows the effect of the dust-to-gas mass ratio. Here we adopt the mean hydrogen density of 3 cm^{-3} to avoid having a too small disc optical depth for the case of $\mathcal{D} = 10^{-3}$, otherwise we have almost zero attenuation at visual band which is the normalization of the presentation. We find that a steeper attenuation law as \mathcal{D} decreases because the disc optical thickness decreases. Conversely, we can make a grayer attenuation law if \mathcal{D} increases. However, it is unlikely that many galaxies have a much higher dust-to-gas ratio than that of the Milky Way.

5.1.7 Global geometry

We examine the effect of the global geometry. Suppose a sphere having a two-phase medium with an equilibrium thermal pressure and a mean gas density. Young stars are confined in clumps, and clumps and older stars distribute uni-

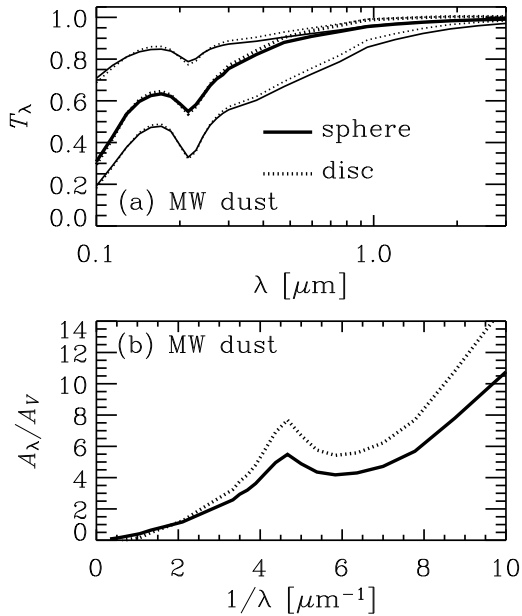


Figure 11. Comparison with a disc geometry and a spherical geometry: (a) transmission rates and (b) attenuation laws normalized at visual band. The solid curves are the spherical case and the dotted curves are the disc case. The thin curves in the panel (a) are transmission rates T_0 (upper) and T_1 (lower). The thick curves in both panels are the composite transmission rates/attenuation laws. The Milky Way type dust is assumed.

formly in the sphere. When we consider isotropic scatterings and assume that the scattered photons are also distributed uniformly in the sphere, the transmission rate for diffuse sources can be analytically expressed as equation (10) with the effective optical depth of $\kappa_{\text{eff}}R$ and the effective albedo ω_{eff} . The radius of the sphere R is set to be equal to the dusty disc h_d for the comparison. The clump optical depth and albedo are also given by equations (3) and (9). Therefore, we have the transmission rate of the clumpy sphere as

$$T^{\text{sph}} = f_y T_1^{\text{sph}} + (1 - f_y) T_0^{\text{sph}}, \quad (25)$$

where the transmission rate for the diffuse source is

$$T_0^{\text{sph}} = P_{\text{esc}}(\kappa_{\text{eff}}h_d, \omega_{\text{eff}}), \quad (26)$$

and the transmission rate for the clumpy source is

$$T_1^{\text{sph}} = P_{\text{esc}}(\tau_{\text{cl}}, \omega_{\text{cl}}) P_{\text{esc}}(\kappa_{\text{eff}}h_d, \omega_{\text{eff}}). \quad (27)$$

Figure 11 shows the comparison of the disc and spherical geometries. We have assumed the standard set tabulated in table 1 in this comparison. For the disc geometry, we adopted $\xi = 0.5$ since this choice is not so important as shown in section 5.1.2. We find very similar transmission rates. Differences appear in longer wavelengths where the optical depth is small. This differences are caused by the scattering. In the face-on disc geometry, the path length of the photons scattered into the observer's (face-on) line of sight is shorter than the original length. On the other hand, the scattered path length is longer than the original one in the spherical geometry. Thus, the face-on disc is more

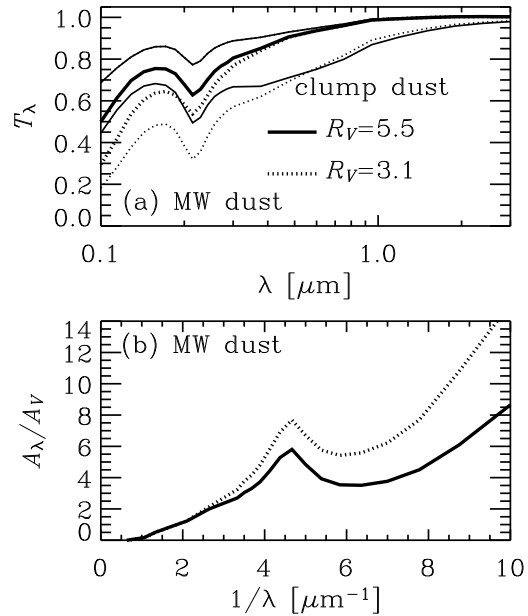


Figure 12. Different dust property in clumps: (a) transmission rates and (b) attenuation laws normalized at visual band. The solid curves are the case that the extinction law of $R_V = 5.5$ is assumed only for dust in clumps, and the dotted curves are the case that the clump dust is the same as the diffuse dust ($R_V = 3.1$). The thin curves in the panel (a) are transmission rates T_0 (upper) and T_1 (lower). The thick curves in both panels are the composite transmission rates/attenuation laws. The Milky Way type dust is assumed.

transparent for the scattered photons than the spherical geometry. This leads to the difference of the attenuation law normalized at visual band because of the different normalization.

5.1.8 Grayer dust in clumps

The observed extinction laws in the Milky Way and Magellanic Clouds show a very large variety among lines of sight and are expected to depend on the environment (e.g., Fitzpatrick 1999; Gordon et al. 2003). Especially, the dust property in star-forming regions (i.e. clumps) may be different from that in diffuse medium. Indeed, Cardelli, Clayton, & Mathis (1989) showed that the extinction laws along some lines of sight toward dense clouds have a large value of $R_V \equiv A_V/E(B - V)$; a grayer extinction law. For example, they found $R_V = 5.5$ toward the Orion nebula, in contrast, $R_V = 3.1$ for the average extinction law. Such a large R_V was attributed to the grain growth in dense medium. On the other hand, Rachford et al. (2002) reported that there is no correlation between R_V and the molecular fraction along translucent lines of sight. Although a systematic difference of the dust property in dense medium (a grayer extinction law) is not completely established, the possible effect is worth examining.

We assume that the dust in clumps is grayer than the diffuse dust; the extinction cross section ($k_{d,\lambda}$) in clumps is set to be the extinction law with $R_V = 5.5$ by Cardelli et

al. (1989). The extinction cross section for the inter-clump dust is the same as introduced in section 3.1. This corresponds to the case of $R_V = 3.1$. The scattering albedo ($\omega_{d,\lambda}$) and the asymmetry parameter ($g_{d,\lambda}$) are not changed because we do not have enough informations about them for the case of $R_V = 5.5$. If the dust size of $R_V = 5.5$ is larger than that of $R_V = 3.1$, the adopted scattering albedo for $R_V = 5.5$ may be smaller than the real values in optical wavelengths. It leads a underestimation of the transmission rate T_1 . However, the composite attenuation at the visual band is dominated by T_0 which is determined by the $R_V = 3.1$ dust. Thus, the effect is not important.

Figure 12 shows the case assuming the grayer dust of $R_V = 5.5$ in clumps as solid curves. For the dotted curves, the clump dust is the same as the diffuse dust which has always $R_V = 3.1$. From the top panel, we find that the transmission rate T_1 of $R_V = 5.5$ becomes larger and grayer than that of $R_V = 3.1$. This makes the composite attenuation law grayer (bottom panel). However, it is still steeper than the extinction law (of $R_V = 3.1$) and the Calzetti law.

5.2 Calzetti law

The attenuation law obtained by Calzetti et al. (1994) from observations of the UV bright starburst galaxies is grayer than the extinction laws of the Milky Way and the Magellanic Clouds. Here we try to reproduce the Calzetti law in the framework of this paper: the attenuation law through the two-phase ISM and the age-selective attenuation.

Although we have obtained a steep attenuation law for normal disc galaxies in section 4, we can also make a grayer attenuation law as seen in section 5.1, for example, a larger mean density. Figure 13 shows a good agreement between the Calzetti law (dotted) with our composite attenuation law for the face-on case with a mean hydrogen density of $5\text{--}10\text{ cm}^{-3}$ (solid). Active star-forming galaxies are likely to have a large amount of gas, and the gas density should exceed a certain critical value (Kennicutt 1989). The hydrogen density of $5\text{--}10\text{ cm}^{-3}$ corresponds to $50\text{--}100 M_\odot\text{pc}^{-2}$ for the disc half height of 150 pc. Indeed, this gas column density greatly exceeds the critical density for the star formation found by Kennicutt (1989).

There are two alternative ways to reproduce the Calzetti law by our model: a highly inclined disc and a system dominated by young stars. Even in the case of the mean hydrogen density of 1 cm^{-3} , the composite attenuation laws with an inclination angle of $75\text{--}80^\circ$ (dashed curves in figure 13) also show a good agreement with the Calzetti law. However, this is unlikely because there is no systematic bias toward very high inclinations in the sample galaxies of Calzetti et al. (1994). Since the galaxies really show an active star formation, the luminosity may be dominated by young stars. In this case, the attenuation law with $f_y = 1$ (i.e. attenuation law produced only by T_1) is suitable. The dot-dashed curves show such cases with a mean hydrogen density of $3\text{--}10\text{ cm}^{-3}$ (face-on). Again, a larger density is preferred.

5.3 Charlot and Fall prescription

Charlot & Fall (2000) proposed a simple prescription of the

attenuation law with the age-selective attenuation and explained a lot of observational properties of the UV bright starburst galaxies. They adopted the age-selective attenuation by a similar way to us: the optical depth for old stars is only that by dust diffusely distributed in the ISM τ_{ISM} and the optical depth for young stars is the sum of τ_{ISM} and the optical depth by dust in the birth cloud τ_{BC} . Then, they simply assumed that the wavelength dependences of τ_{ISM} and τ_{BC} are the same: $\lambda^{-0.7}$. We examine this point.

In figure 14, we show the normalized attenuation laws for T_1 (dashed) and T_0 (dotted) with several mean hydrogen densities, and compare them with the power-law attenuation with the index -0.7 (solid) proposed by Charlot & Fall (2000). We find that (1) the slopes of the attenuation laws for the embedded young stars (T_1) and for the diffuse stars (T_0) are not the same. (2) The slopes decreases, especially for the diffuse stars, as the mean gas density increases. (3) The slopes for both stellar populations are similar to each other in a case with a mean hydrogen density of $\sim 5\text{ cm}^{-3}$, in which the composite attenuation law is also similar to the Calzetti law. Therefore, the Charlot and Fall prescription and also the Calzetti law can be interpreted as a special case of a larger density (i.e. starburst) disc in the framework presented here.

6 CONCLUSION

The attenuation laws through the interstellar medium (ISM) with clumpy distributions of stars and dust was investigated in this paper. As an application of the multi-phase ISM model, we introduced a physical model of the clumpiness of the medium (i.e. dust distribution). In the model, the two parameters determining the clumpiness, the density contrast between clumps and the inter-clump medium and the volume filling fraction of clumps, were translated into two physical quantities in the ISM: the equilibrium thermal pressure and the mean gas density. The radiative transfer through the clumpy ISM was treated in a 1-D plain-parallel geometry by the mega-grain approximation developed by Városi & Dwek (1999). For the clumpiness of the stellar distribution, we considered two stellar populations: older stars diffusely and smoothly distributed in the medium and younger stars embedded in clumps (i.e. birth clouds). This provides the age-selective attenuation (Silva et al. 1998); young stars are surrounded by a denser dusty medium and suffer a stronger attenuation. The transmission rate of the entire radiation from the two stellar populations is a composite of the transmission rates of each individual population with a luminosity weight. The stellar population dominating the radiation changes from older stars to younger stars as the wavelength decreases. With this fact, the age-selective attenuation makes the attenuation law steep; the composite attenuation rapidly increases from small attenuation for older stars at a long wavelength to large attenuation for younger stars at a short wavelength. Therefore, the attenuation law expected for normal disc galaxies is much steeper than the Calzetti law (Calzetti et al. 1994) and the extinction laws in the Milky Way and the Magellanic Clouds. After an extensive survey of the parameter space, it was shown that the steep attenuation law is very robust for the parameter set expected in normal disc galaxies. Furthermore, the Calzetti

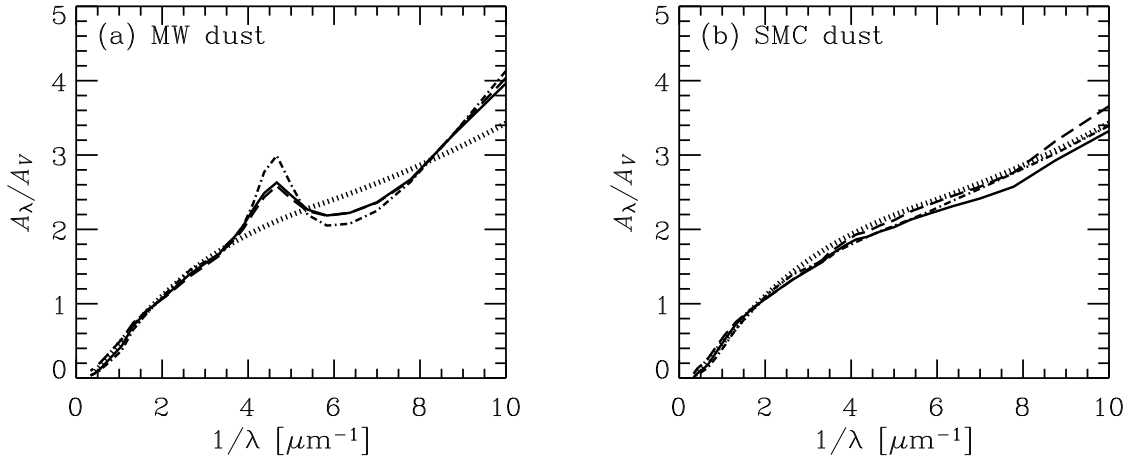


Figure 13. Comparison of the attenuation laws with the Calzetti law: (a) Milky Way type dust and (b) Small Magellanic Cloud type dust. The dotted curve is the Calzetti law. The solid curves are the composite attenuation laws for the face-on case with the mean hydrogen number densities of (a) 5.5 cm^{-3} and (b) 8.9 cm^{-3} . The dashed curves are the composite attenuation laws of the mean hydrogen density of 1 cm^{-3} for the inclination angle of (a) 76.9° and (b) 80.7° . The dot-dashed curves are the face-on attenuation law for T_1 with the mean hydrogen densities of (a) 3.4 cm^{-3} and (b) 8.9 cm^{-3} .

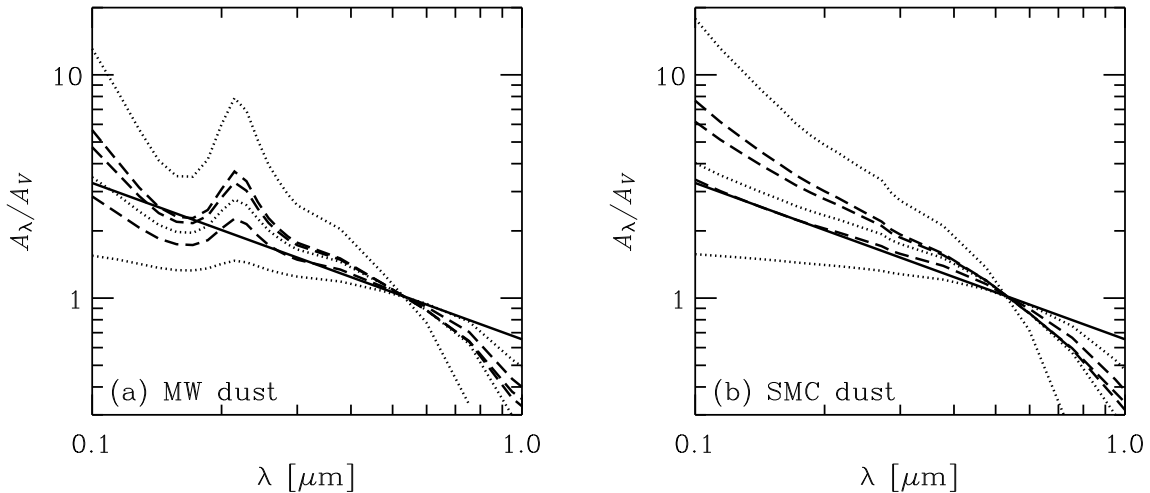


Figure 14. Comparison of attenuation laws with the prescription by Charlot & Fall (2000): (a) Milky Way type dust and (b) Small Magellanic Cloud type dust. The solid line is the power-law attenuation law by Charlot & Fall (2000); $A_\lambda \propto \lambda^{-0.7}$. The dotted and dashed curves are the attenuation laws corresponding transmission rates T_0 and T_1 , respectively. The mean hydrogen number densities are 0.51 , 2.1 , and 8.9 cm^{-3} from top to bottom for both types of curves and in both panels.

law was reproduced in the framework presented here with a larger gas density than that in normal disc galaxies. Such a large gas density is very likely for the starburst galaxies. Finally, we examined the validity of a simple prescription of the attenuation law proposed by Charlot & Fall (2000). Then, we found that their prescription (and also the Calzetti law) is a special case with a larger density disc in our model.

Interestingly, the UV color (or spectral slope) of normal disc galaxies is systematically redder than that of UV bright starbursts at a fixed flux ratio of the UV to the infrared (or fixed UV attenuation) (e.g., Bell 2002). A first result of GALEX also shows such trend (Buat et al. 2005). One of the explanations of the trend is that normal disc

galaxies have intrinsically red colors because of their quiescent star-forming activity (Kong et al. 2004). However, a steep attenuation law presented here can make galaxies red with small attenuation, and then, can be an alternative interpretation of the trend. Nowadays, GALEX is providing us with the UV data, including spectra, of a large number of normal disc galaxies. In the near future, GALEX will conclude whether the attenuation law of normal disk galaxies is steep or not.

ACKNOWLEDGMENTS

The author thanks Taishi Nakamoto, Tsutomu T. Takeuchi, Pasquale Panuzzo, Veronique Buat, Denis Burgarella, Jean-Michel Deharveng, Hideyuki Kamaya, Toshinobu Takagi, and Nobuo Arimoto for discussions and encouragements. The author also thanks the anonymous referee for useful suggestions. The author is supported by the JSPS Postdoctoral Fellowships for Research Abroad.

REFERENCES

- Baes, M., Dejonghe, H., 2001a, MNRAS, 326, 722
 Baes, M., Dejonghe, H., 2001b, MNRAS, 326, 733
 Bell, E. F., 2002, ApJ, 577, 150
 Bianchi, S., Ferrara, A., Davies, J. I., Alton, P. B., 2000, MNRAS, 311, 601
 Binney, J., Merrifield, M., 1998, Galactic Astronomy, Princeton University Press, NJ
 Blitz, L., Shu, F. H., 1980, ApJ, 238, 148
 Boulares, A., Cox, D. P., 1990, ApJ, 365, 544
 Bruzual, A. G., Magris, G. C., Calvet, N., 1988, ApJ, 333, 673
 Buat, V., Bugarella, D., Deharveng, J.-M., Kunth, D., 2002, A&A, 393, 33
 Buat, V., Iglesias-Páramo, J., Seibert, M., Burgarella, D., et al., 2005, ApJ, 619, L51
 Calzetti, D., 2001, PASP, 113, 1449
 Calzetti, D., Kinney, A. L., Storchi-Bergmann, T., 1994, ApJ, 429, 582
 Cardelli, J. A., Clayton, G. C., Mathis, J. S., 1989, ApJ, 345, 245
 Charlot, S., Fall, S. M., 2000, ApJ, 539, 718
 de Bruijne, J. H. J., 1999, MNRAS, 310, 585
 Di Bartolomeo, A., Barbaro, G., Perinotto, M., 1995, MNRAS, 277, 1279
 Draine, B. T., 2003, ApJ, 598, 1017
 Ferrara, A., Bianchi, S., Cimatti, A., Giovanardi, C., 1999, ApJS, 123, 437
 Field, G. B., Goldsmith, D. W., Habing, H. J., 1969, ApJ, 155, L149
 Fischera, J., Dopita, M. A., Sutherland, R. S., 2003, ApJ, 599, L21
 Fischera, J., Dopita, M. A., 2005, ApJ, 619, 340
 Fitzpatrick, E. L., 1999, PASP, 111, 63
 Gordon, K. D., Calzetti, D., Witt, A. N., 1997, ApJ, 487, 625
 Gordon, K. D., Clayton, G. C., Witt, A. N., Misselt, K. A., 2000, ApJ, 533, 236
 Gordon, K. D., Clayton, G. C., Misselt, K. A., Landolt, A. U., Wolff, M. J., 2003, ApJ, 594, 279
 Granato, G. L., Lacey, C. G., Silva, L., Bressan, A., Baugh, C. M., Cole, S., Frenk, C. S., 2000, ApJ, 542, 710
 Heiles, C., Troland, T. H., 2003, ApJ, 586, 1067
 Henyey, L. C., Greenstein, J. L., 1941, ApJ, 93, 70
 Hobson, M. P., Padman, R., 1993, MNRAS, 264, 161
 Kennicutt, R. C., 1989, ApJ, 344, 685
 Kong, X., Charlot, S., Brinchmann, J., Fall, S. M., 2004, MNRAS, 349, 769
 Koyama, H., Inutsuka, S.-I., 2000, ApJ, 532, 980
 Larson, R. B., 1981, MNRAS, 194, 809
 Leitherer, C., Li, I.-H., Calzetti, D., Heckman, T. M., 2002, ApJS, 140, 303
 Martin, D. C., Fanson, J., Schiminovich, D., Morrissey, P., et al., 2005, ApJ, 619, L1
 Matthews, L. D., Wood, K., 2001, ApJ, 548, 150
 McKee, C. F., Ostriker, J. P., 1977, ApJ, 218, 148
 Mihalas, D., Weibel-Mihalas, B., 1999, Foundations of Radiation Hydrodynamics, Dover, New York
 Myers, P. C., 1978, ApJ, 225, 380
 Natta, A., Panagia, N., 1984, ApJ, 287, 228
 Neufeld, D. A., 1991, ApJ, 370, L85
 Ng, K.-C., 1974, J. Chem. Phys., 61, 2680
 Olson, G. L., Auer, L. H., Buchler, J. R., 1986, JQSRT, 35, 431
 Pierini, D., Gordon, K. D., Witt, A. N., Madsen, G. J., 2004, ApJ, 617, 1022
 Rachford, B. L., Snow, T. P., Tumlinson, J., Shull, J. M., et al., 2002, ApJ, 577, 221
 Silva, L., Granato, G. L., Bressan, A., Danese, L., 1998, ApJ, 509, 103
 Spitzer, L., 1978, Physical Processes in the Interstellar Medium, Wiley, New York
 Tuffs, R. J., Popescu, C. C., Völk, H. J., Kylafis, N. D., Dopita, M. A., 2004, A&A, 419, 821
 Városi, F., Dwek, E., 1999, ApJ, 523, 265
 Witt, A. N., Gordon, K. D., 1996, ApJ, 463, 681
 Witt, A. N., Gordon, K. D., 2000, ApJ, 528, 799
 Wolfire, M. G., Hollenbach, D., McKee, C. F., Tielens, A. G. G. M., Bakes, E. L. O., 1995, ApJ, 443, 152
 Wolfire, M. G., McKee, C. F., Hollenbach, D., Tielens, A. G. G. M., 2003, ApJ, 587, 278